RESEARCH ARTICLE

Ethnoracial disparities in gray matter atrophy are mediated by structural disconnectivity in multiple sclerosis

Ahmed Bayoumi[1] (iD), Joseph A. Thomas[1], Breanna R. Alonzo[1,#], Juan Jimenez[1,#], Christopher M. Orlando[2], Carlos A. Pérez[3], Khader M. Hasan[4], Jerry S. Wolinsky[1] (iD) & John A. Lincoln[1] (iD)

[1]Department of Neurology, McGovern Medical School at UTHealth, Houston, Texas, USA
[2]Department of Neurology, University of Southern California Keck School of Medicine, Los Angeles, California, USA
[3]Department of Neurology, Baylor College of Medicine, Houston, Texas, USA
[4]Department of Diagnostic and Interventional Imaging, McGovern Medical School at UTHealth, Houston, Texas, USA

Correspondence

Ahmed Bayoumi, Department of Neurology, McGovern Medical School at UTHealth, 6431 Fannin St, Houston, TX 77030, USA. Tel: +1 (713) 500-7029; Fax: +1 (713) 512-2239; E-mail: ahmed.bayoumi@uth.tmc.edu

#These authors contributed equally to this work.

Abstract

Objective: To investigate ethnoracial disparies in gray matter (GM) atrophy, the contribution of white matter lesions and consequent structural disconnectivity among patients with multiple sclerosis (MS). **Methods**: This retrospective study included 297 patients with MS (pwMS), 98 Hispanic/Latinx (H-MS), 82 non-Hispanic Black (B-MS), and 117 non-Hispanic White (W-MS). GM atrophy was assessed using univariate, voxel-based morphometry, and multivariate techniques, source-based morphometry. Structural disconnectivity secondary to white matter lesions was evaluated using the network modification tool. Mediation analyses explored relationships between ethnoracial groups, white matter lesions, structural disconnectivity, and gray matter atrophy. **Results**: B-MS and H-MS generally exhibited greater gray matter atrophy compared to W-MS, particularly in temporal, parahippocampal, precuneus, and cuneus GM. Structural disconnectivity differences were most prominent in the hippocampal, cingulate, precuneus, and deep gray matter regions. Mediation analyses revealed that lesion load significantly mediated group differences in global GM atrophy (percent mediated = 52.4%), while structural disconnectivity mediated some differences in specific gray matter components, notably in deep gray matter, insular, and anterior cingulate regions. **Interpretation**: Significant ethnoracial disparities exist in GM atrophy and its patterns among diverse MS patients, partially mediated by white matter lesions and consequent structural disconnectivity. These findings underscore the importance of considering ethnoracial factors in MS research and clinical practice, potentially informing personalized treatment strategies and emphasizing the need for diverse representation in clinical trials.

Introduction

Multiple sclerosis (MS) is the most prevalent chronic neurologic disease in young adults in the United States (US),[1] and a leading cause of non-traumatic disability.[2] Recent studies have shown how MS is more prevalent among minority populations than previously thought,[3] highlighting significant ethnoracial disparities. Non-Hispanic Black (B-MS) and Hispanic/Latinx (H-MS) patients with MS (PwMS) often present earlier, with greater disease burden and faster disability accumulation compared to non-Hispanic White (W-MS) PwMS.[4–7] Imaging studies have shed light on some of the structural underpinnings of such disparities. B-MS and H-MS were previously reported to have higher cortical gray matter (GM) atrophy relative to W-MS, most pronounced in temporal and parietal regions in B-MS. H-MS were also shown to have greater Deep GM (DGM) atrophy.[8,9] Moreover, B-MS and W-MS were shown to have greater inflammatory white matter (WM) lesion burden compared to W-MS, especially periventricularly and infratentorially.[10] It is thought that a host of biological,

genetic, and sociocultural factors contribute to the observed disparities.[11]

MS pathology is characterized by concomitant neuroinflammation and neurodegeneration, manifesting as focal demyelination, axonal disruption, and brain atrophy.[12] GM atrophy, a chief correlate of physical disability and cognitive decline in PwMS, appears early and worsens with disease progression.[13,14] Various mechanisms are thought to contribute to GM neuroaxonal loss, including retrograde degeneration secondary to WM lesions, focal cortical demyelination,[15–18] and DGM degeneration, with thalamic atrophy serving as a significant marker of neurodegeneration due to its role as a central hub in brain networks.[19] Voxel-based morphometry[20] (VBM) quantifies and analyzes regional GM atrophy using magnetic resonance imaging (MRI), which can be particularly useful in deriving group-level insights.[21,22] It has shown regional GM loss in PwMS which correlates with disease duration and severity,[23] though its univariate approach analyzing voxels independently limits its ability to distinguish between different atrophy patterns, which can be clinically relevant in PwMS.[24,25] An alternative multivariate data-driven technique, source-based morphometry (SBM), pools signals across different voxels exhibiting covariance within brain regions using independent component analysis (ICA).[26]

However, while these techniques provide valuable insights into GM atrophy, they do not address the relationship between white matter lesions and GM atrophy. MS-related WM lesions disrupt brain networks, leading to structural disconnectivity that correlates with both GM pathology and clinical outcomes.[27,28] The Network Modification tool (NeMo) quantifies this disconnectivity by estimating WM pathway disruption and GM disconnection using the Human Connectome Project normative dataset,[29] demonstrating comparable utility in predicting clinical disability in PwMS relative to diffusion MRI measures.[28] To untangle the complex relationships between multiple outcome-related variables, mediation analysis provides a statistical framework for understanding how variables may influence each other. This approach helps determine whether the effect of one variable on another occurs directly or indirectly through an intermediary variable (mediator), offering insights into the possibly contributing mechanisms.[30] It has been recently used to investigate the mediating role of paramagnetic rim lesions on the relationship between race and disability in PwMS.[31]

We aimed to investigate ethnoracial disparities in gray matter (GM) atrophy in PwMS in a large single-center cohort, testing the following hypotheses: (1) B-MS, H-MS, and W-MS exhibit different extent and patterns of GM atrophy; (2) WM lesion burden and resultant structural disconnectivity mediate these ethnoracial differences in GM atrophy.

Methods

Subjects

Demographic, clinical, and imaging data were obtained under human research and subject protocol approved by the McGovern Medical School at UTHealth institutional review board. This retrospective study included patients with MS diagnosis, seen between May 2009 and August 2022 at the comprehensive MS care clinic at UT Physicians. MS diagnosis was initially identified by ICD-9 (340) and/or ICD-10 (G35) codes, subsequently individual clinical, radiological, and laboratory data were reviewed by two MS specialists (C.A.P. and J.A.L.) to confirm dissemination in time and space meeting the 2017 McDonald diagnostic criteria. Previous publications describe the studied cohort in detail.[6,7,9] Inclusion criteria included MRI scans obtained within one month of the clinical evaluation visit and the absence of brain trauma or other demyelinating central nervous system conditions upon record review. Exclusion criteria included patients with incomplete medical records, lacking MRI data, or patients with MRI data obtained within 30 days of a clinically documented relapse, corticosteroid administration, and/or disease-modifying therapy (DMT) switching. Demographic and clinical data were extracted as previously described[9] from medical records including age, sex, disease duration, treatment delay (time interval between first clinical symptom onset and DMT initiation), disease phenotype, Expanded Disability Status Score (EDSS), DMT, body mass index (BMI), and other comorbidities as evidenced by diagnosis codes or corresponding pharmacotherapy. Subjects were divided into three groups according to their self-reported race/ethnicity: B-MS, H-MS, and W-MS. We initially selected equal numbers of patients, 100, across the three groups (1:1:1), of frequency matching was used to ensure comparable distributions of age and sex across the groups.

Image acquisition

MRI was performed on a single 3.0 T Philips Ingenia research scanner with a maximum gradient amplitude of 45 mT/m and a 15-channel SENSE-compatible head coil (Philips Medical Systems, Best, Netherlands). High-resolution 3D T_1-weighted (T_1-w) magnetization prepared rapid gradient echo images (voxel size: $1 \times 1 \times 1$ mm^3, field-of-view (FOV): 256×256 mm^2, repetition time/echo time: 8/3.7 msec), as well as T_2-weighted

fluid-attenuated inversion recovery (T$_2$-w FLAIR) images (voxel size: $1 \times 1 \times 1$ mm^3, FOV: 256×256 mm^2, repetition time/echo time: 4800/300 msec, and inversion time: 1650 msec) were acquired.

Image analysis

An overview of the image processing workflow is illustrated in Figure 1. Details on the image analysis methods can be found in the Supplementary Materials.

Preprocessing and lesion segmentation

In FSL (version 6.0.6, FMRIB Software Library; http://www.fmrib.ox.ac.uk/fsl), T$_1$-w and T$_2$-FLAIR images were bias-field corrected and co-registered. WM hyperintense lesions were segmented on the T1-w and T2-w FLAIR images estimating total lesion distribution and volume, as well as labeled regional volumes (periventricular, subcortical, juxtacortical, and infratentorial) using the Lesion Segmentation Toolbox.[32] Produced lesion masks were used
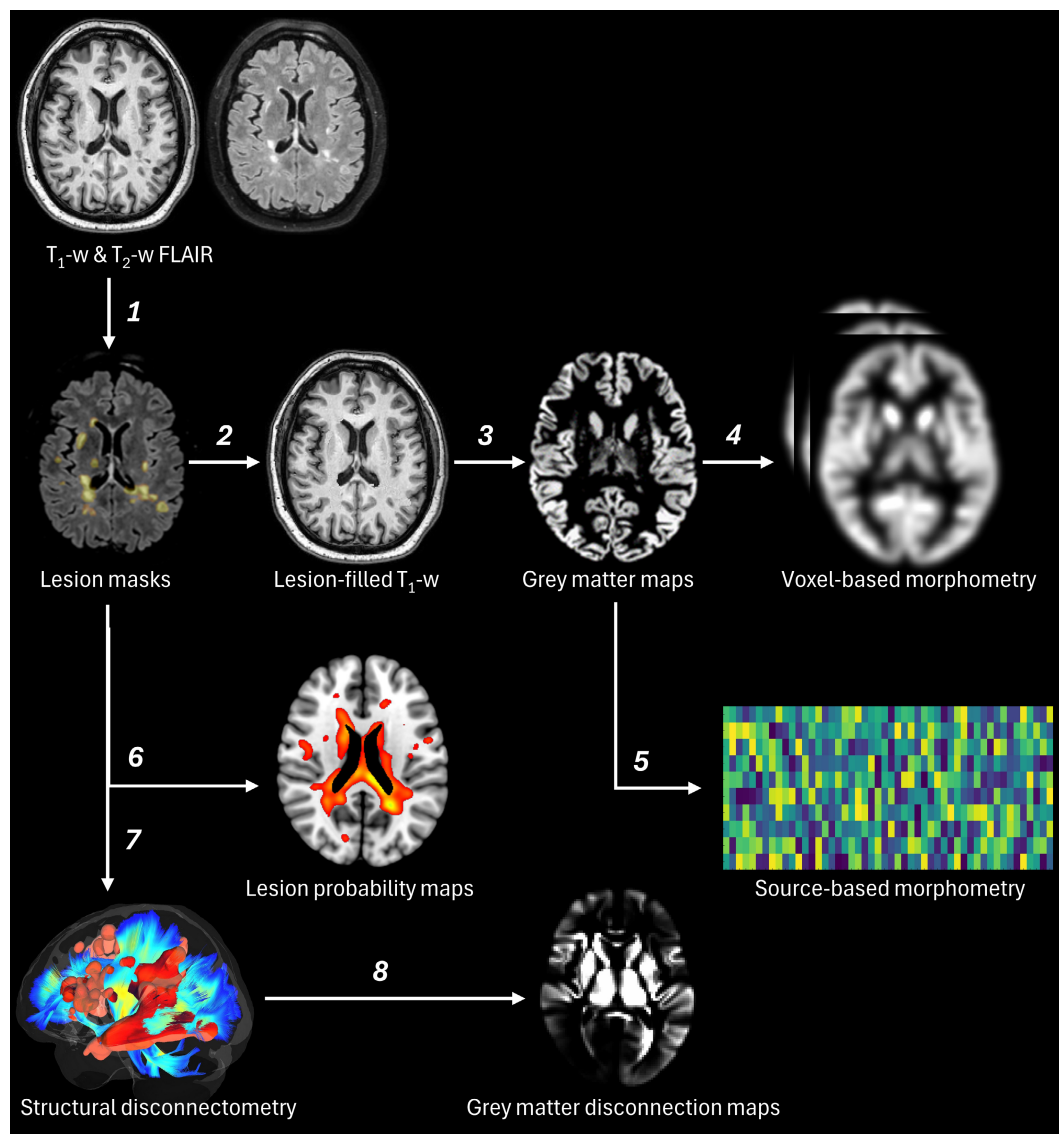

Figure 1. Image analysis workflow. (1) Image co-registration and WM hyperintense lesions segmentation. (2) Inpainting of lesioned voxels on T$_1$-w images. (3) Image normalization and tissue class segmentation. (4) Univariate analysis of GM group differences. (5) Multivariate analysis of GM group differences. (6) Mean group lesion distribution and their differences. (7) Quantification of interrupted white matter fibers attributed to lesion distribution. (8) Calculation of regional gray matter disconnection secondary to lesion-related white matter fiber interruption.

to fill T_1-w images[33] to mitigate the effect of lesioned voxels on image normalization.[34] The produced lesion masks and the quality of the filled T_1-w images were visually assessed.

GM assessment

We utilized complementary techniques to comprehensively evaluate GM differences across the studied groups. VBM was utilized as a univariate method to assess overall differences in global GM atrophy, and SBM was used to provide insights on topographically co-occurring GM loss shedding light on the atrophy patterns.

VBM

The lesion-filled T_1-w images were processed using the standard Computational Anatomy Toolbox 12 (CAT12; https://neuro-jena.github.io/cat) pipeline, which has been validated in cross-sectional MS studies and shown to provide robust segmentations.[34,35] The images were registered to standard space and segmented, estimating total intracranial (TIV), GM, WM volumes, and the different brain tissue maps including the modulated normalized GM maps. The T_1-w images and produced GM maps were assessed for image quality and sample inhomogeneity, outliers ($>\pm2$ standard deviations) were excluded from the analysis.[36] Groups were compared for regional GM differences including age, sex, and TIV as covariates. After probabilistic threshold-free cluster enhancement,[37] results were produced controlling for false discovery rate (FDR).

SBM

To investigate GM regions with covarying atrophy, the GIFT toolbox (https://github.com/trendscenter/gift) was used. We estimated the number of components[26] and performed independent component analysis using the Infomax algorithm[38] on the modulated normalized GM maps. The reliability of the identified GM components (GMCs) was ensured using 100-fold cross-validation in ICASSO (https://research.ics.aalto.fi/ica/icasso/). Subjects' loading coefficients for the GMCs were obtained and converted to Z-scores.

Structural disconnectometry

NeMo[29] was used to calculate the change in connectivity (ChaCo) scores to the different GM regions. The standardized lesion masks were used to define the subsequent pattern of structural disconnectivity as the percentage of tractography streamlines connected to the region intersecting with the lesion mask. The target GM regions used were whole-brain GM atlas parcellations as well as the identified gray matter patterns, GMCs, obtained using SBM.

Statistical analysis

Statistical analyses were conducted in *jamovi* (Version 2.3, https://www.jamovi.org/), *p*-values < 0.05 were considered significant. *P*-values were adjusted for FDR using the Benjamini–Hochberg procedure when appropriate. Continuous demographic, clinical, and imaging variables were assessed for normality of distribution using Q-Q plots and equal variances using Levene's test. Demographic and clinical variables were compared using analysis of variance (ANOVA), Kruskal–Wallis, and chi-square tests whenever appropriate. GM fraction (GMF) was calculated as total GM volume divided by TIV multiplied by 100, and lesion load (LL) was calculated as total lesion volume divided by TIV multiplied by 1000. Analysis of covariance (ANCOVA) was used to compare the identified GMCs among the ethnoracial groups, controlling for age, sex, and TIV. Partial eta squared (η_p^2) was calculated to estimate the variance explained by ethnoracial group membership, and post-hoc comparisons were conducted using the Games-Howell test. As the structural disconnectivity, ChaCo, scores did not follow normal distribution, the Kruskal–Wallis test was used to calculate group differences. The Dwass–Steel–Critchlow–Fligner test was used to estimate pair-wise differences. Voxel-wise analysis of the WM lesions was conducted estimating group means and differences from 10,000 non-parametric permutations performed using *randomize* in FSL on the standardized lesion masks.

Finally, to examine the relationship between the ethnoracial group, WM lesions/structural disconnectivity, and GM atrophy differences observed among the groups, classical non-parametric mediation analyses were conducted. We examined how ethnoracial group membership affected global GM atrophy via total WM lesion volume, LL, as well as how it affected GMC differences via its corresponding structural disconnectivity secondary to WM lesions. The predictor, ethnoracial group, was used as a categorical independent variable with three contrasts: (1) combined B-MS + H-MS groups vs. W-MS, (2) B-MS vs. W-MS, and (3) H-MS vs. W-MS, with the W-MS group being the reference level. We estimated total, direct and indirect effects (η_p^2), including age, sex, disease duration, clinical phenotype, DMT, and TIV (when appropriate), as covariates, using a maximum likelihood estimator with confidence intervals obtained from 10,000 percentile-corrected bootstraps in a structural equation modeling framework using lavaan.[39] For the first contrast

(B-MS + H-MS vs. W-MS), which had the largest sample size and thus greater statistical power, we calculated the coefficient of determination (R^2) for the direct (R_D^2) and total effects (R_T^2), quantifying the proportion of variance in GM atrophy explained by each. The percent mediation (Pm%) was estimated by dividing indirect effect η_p^2 by total effect η_p^2 multiplied by 100.

Results

Patient characteristics

A total of 316 records were assessed for inclusion, out of which 19 outliers were excluded (2 from B-MS, 10 from W-MS, and 7 from H-MS). The analysis included 297 PwMS, divided into three groups: B-MS ($n = 82$, mean age = 39.3 ± 10.5 years, 79.3% female), W-MS ($n = 117$, mean age = 40.8 ± 12.5 years, 71.8% female), and H-MS ($n = 98$, mean age = 37.4 ± 11.6 years, 76.5% female). Table 1 summarizes demographic, clinical and imaging data for included subjects. The three groups did not show significant differences in MS disease duration (B-MS: mean disease duration = 6.9 ± 6.2 years, W-MS: mean disease duration = 6.9 ± 7.9, and H-MS: mean disease duration = 6.3 ± 7.3 years, $p = 0.4$), treatment delay, EDSS, disease phenotype, DMT, or other comorbidities. Total gray matter fraction was significantly lower in B-MS and H-MS compared to W-MS (B-MS: $43.7 \pm 3.6\%$, W-MS: $45.2 \pm 3.1\%$, and H-MS: $44.8 \pm 3.5\%$, $p = 0.02$), and lesion load was greater (B-MS: 13.0 ± 15.9 mL, W-MS: 5.6 ± 8.3 mL, and H-MS: 10.5 ± 13.3 mL, $p < 0.001$). Figure 2 depicts the lesion probability maps for each group and their differences. Compared to W-MS, B-MS and H-MS had significantly higher callosal and periventricular lesion volumes, specifically interrupting commissural pathways, forceps minor anteriorly, and forceps major posteriorly, connecting corresponding cortical regions bilaterally as well as association pathways connecting various cortical regions ipsilaterally. More details on the distribution of lesion differences can be found in Table S1.

Univariate GM differences

Figure 3 shows the pairwise regional GM differences among the groups. In general, both B-MS and H-MS groups showed greater GM atrophy relative to W-MS, with more evident atrophy in the B-MS group. B-MS had notable GM decreases in the bilateral lingual, temporal, parahippocampal, precuneus, and cuneus regions when compared to W-MS, meanwhile, H-MS showed the largest decreases in the bilateral fusiform, temporal, lingual, frontal, and parahippocampal regions. Compared to H-

Table 1. Patient demographic, clinical, and imaging characteristics.

	B-MS ($n = 82$)	H-MS ($n = 98$)	W-MS ($n = 117$)	*p*-value
Age (years)	39.3 ± 10.5	37.4 ± 11.6	40.8 ± 12.5	0.1
Sex (% female)	79.3	76.5	71.8	0.5
Disease duration (years)	6.9 ± 6.2	6.3 ± 7.3	6.9 ± 7.9	0.4
Treatment delay[a] (years)	0.3, 1.3	0.6, 1.9	0.6, 3.7	0.06
EDSS[a]	2.0, 2.0	2.0, 2.0	1.5, 2.5	0.3
MS phenotype (%)				0.2
PPMS	11.0	3.1	7.7	
RRMS	81.7	83.7	77.8	
SPMS	7.3	13.3	14.5	
DMT (%)				0.4
Injectable[b]	69.5	57.1	60.7	
Oral[c]	12.2	17.3	16.2	
Infusion[d]	13.4	13.3	16.2	
None	4.9	12.2	6.8	
BMI (kg/m²)	28.4 ± 7.2	28.5 ± 7.2	27.5 ± 7.1	0.5
Smoking (%)				0.5
Current	11.0	6.1	6.8	
Never	79.3	79.6	76.1	
Previous	9.8	14.3	17.1	
Comorbidities (%)				
Hypertension	19.5	32.7	27.4	0.1
Hyperlipidemia	8.5	9.2	9.4	1.0
Diabetes mellitus	7.3	6.1	4.3	0.6
GMF (%)	43.7 ± 3.6	44.8 ± 3.5	45.2 ± 3.1	**0.02**
WMF (%)	36.1 ± 2.9	35.7 ± 2.8	36.1 ± 2.5	0.5
Lesion load (mL)	13.0 ± 15.9	10.5 ± 13.3	5.6 ± 8.3	**<0.001**
Periventricular	14.9 ± 19.3	12.0 ± 17.0	6.3 ± 10.5	**<0.001**
Subcortical	0.3 ± 0.3	0.3 ± 0.4	0.3 ± 0.3	0.8
Juxtacortical	1.3 ± 1.5	1.3 ± 1.8	0.9 ± 1.4	0.1
Infratentorial	0.2 ± 0.2	0.2 ± 0.4	0.1 ± 0.3	0.5

Listed values are the mean group values and standard deviation where applicable. Bold values indicates *p*-values < 0.05.

BMI, body mass index; B-MS, non-Hispanic Black PwMS group; DMT, disease-modifying therapy; EDSS, expanded disability status scale; GMF, gray matter fraction; H-MS, Hispanic PwMS group; MS, multiple sclerosis; PPMS, primary progressive multiple sclerosis; RRMS, relapsing-remitting multiple sclerosis; SPMS, secondary progressive multiple sclerosis; WMF, white matter fraction.; W-MS, non-Hispanic White PwMS group.

[a]Median and interquartile range are represented.

[b]Injectable DMTs: glatiramer acetate, interferon beta-1a, interferon beta-1b, and peginterferon beta-1a.

[c]Oral DMTs: diroximel fumarate, dimethyl fumarate, teriflunomide, fingolimod, and siponimod.

[d]Infusion DMTs: ocrelizumab, natalizumab, alemtuzumab, rituximab, and intravenous immunoglobulin (IVIG).

MS, B-MS also showed decreases in the bilateral cuneus, orbital, precuneus, and occipital regions. Whereas no areas showed significant decreases in W-MS compared to
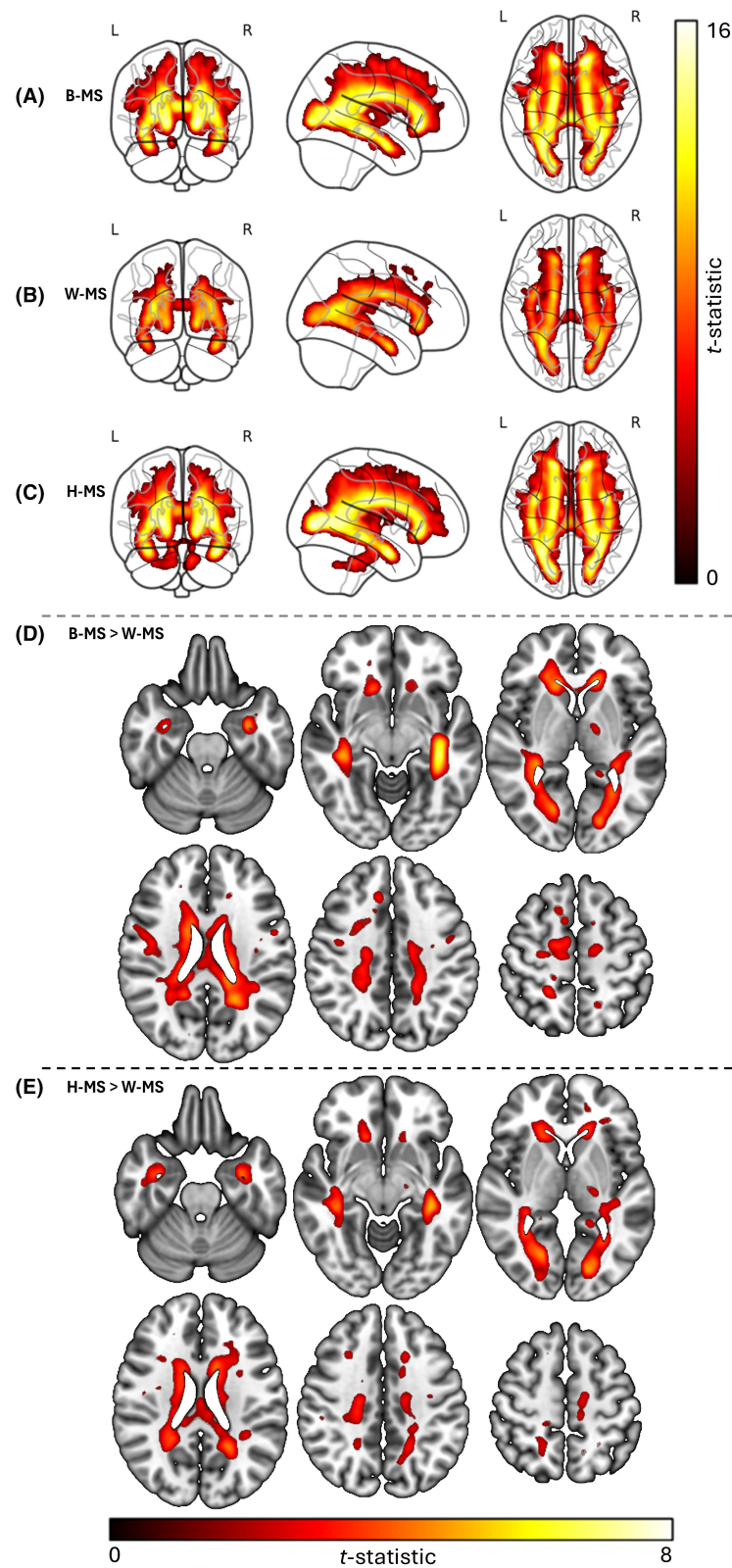
Figure 2. Lesion probability maps and their group differences. (A–C) represent lesion probability maps for each group estimated using non-parametric voxel-wise statistics in B-MS, W-MS, and H-MS respectively. (D and E) represent group differences in lesion distribution between B-MS versus W-MS (D), and H-MS versus W-MS (E). Higher *t*-values denote higher probabilities.
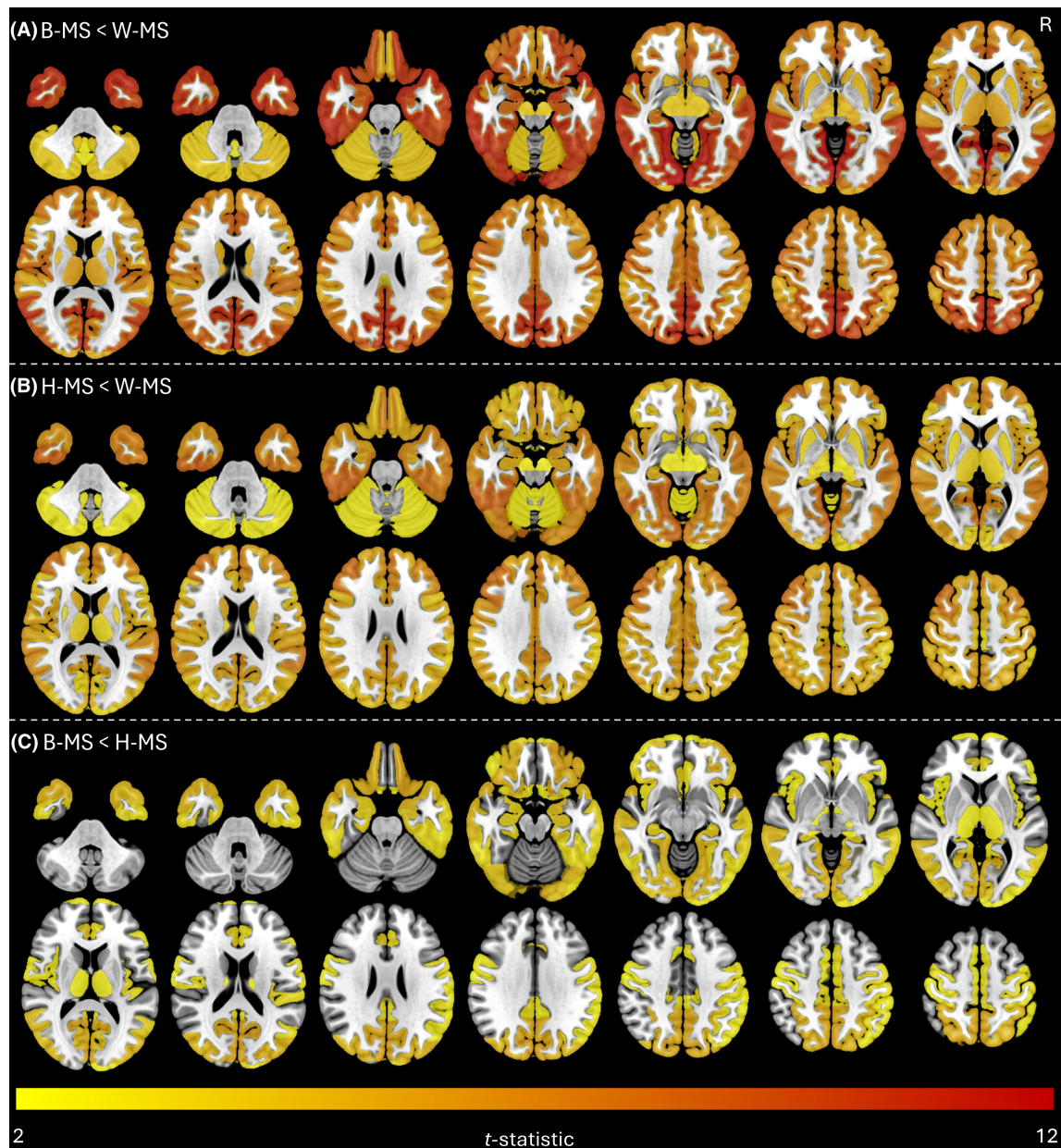

Figure 3. Univariate gray matter group differences. Pair-wise differences in gray matter estimated using VBM depicting areas with more pronounced gray matter atrophy in B-MS relative to W-MS (A), H-MS relative to W-MS (B), and B-MS relative to H-MS (C). Higher *t*-values denote larger differences.

B-MS and H-MS, and no areas showed significant decreases in H-MS compared to B-MS. Detailed results showing pair-wise regional GM differences statistics found using VBM can be found in Table S2.

Multivariate GM differences

We identified 12 distinct covarying GMCs using SBM, generally corresponding to structurally or functionally

connected regions. The GMCs were labeled using the significantly contributing brain regions, details on their distribution can be found in Table S3. Figure 4 illustrates the identified GMCs and group differences. When comparing the three groups for the identified GMCs, significant differences were found in 9 out of the 12 components. The largest differences were observed in the temporal GMC ($F = 23.1$, $\eta_p^2 = 0.14$, $p_{FDR} < 0.001$), followed by the precuneus ($F = 21.6$, $\eta_p^2 = 0.13$, $p_{FDR} < 0.001$), the posterior cingulate ($F = 19.6$, $\eta_p^2 = 0.12$, $p_{FDR} < 0.001$), then the temporooccipital component ($F = 15.6$, $\eta_p^2 = 0.10$, $p_{FDR} < 0.001$). Post-hoc comparisons revealed that B-MS had the most prominent decreases in the posterior cingulate ($t = -8.5$, $p < 0.001$), the precuneus ($t = -7.8$, $p < 0.001$), and the temporal ($t = -7.6$, $p < 0.001$) components compared to W-MS, meanwhile H-MS showed the greatest decreases in the temporooccipital ($t = -5.9$, $p < 0.001$), posterior cingulate ($t = -3.8$, $p < 0.001$), and frontal ($t = -3.6$, $p = 0.001$) components compared to W-MS. Results are detailed in Table 2.

Lesion-driven structural disconnectivity

Figure 5 shows the pairwise differences in structural disconnectivity to regional GM. Overall, the largest differences were observed in the hippocampus, cingulate, and precuneus as well as deep gray matter connectivity, detailed results can be found in Table S4. Furthermore, we computed the change in connectivity to the GMCs identified using SBM shown in Table 2. The largest differences in structural disconnectivity secondary to lesions were observed in the anterior cingulate ($\chi^2 = 11.1$, $p_{FDR} = 0.02$), posterior cingulate ($\chi^2 = 11.2$, $p_{FDR} < 0.05$), and DGM ($\chi^2 = 10.6$, $p_{FDR} = 0.02$) components.

Mediation effects of structural disconnectivity on GM atrophy differences

The analyses examined how lesion load and structural connectivity possibly influenced ethnoracial differences in GM atrophy. For the combined minority groups comparison (B-MS + H-MS vs. W-MS, Table 3), total lesion load significantly mediated differences in global GM fraction, accounting for 52.4% of the total effect (total effect $\eta_p^2 = -1.43$, $p < 0.001$; direct effect $\eta_p^2 = -0.68$, $p < 0.05$; indirect effect $\eta_p^2 = -0.75$, $p < 0.001$). Meanwhile, structural disconnectivity had varying impact across the GMCs, with the strongest mediation observed in DGM (Pm = 82.9%), followed by insular (Pm = 29.6%) and anterior cingulate (Pm = 24.3%), and temporal components (Pm = 9.7%).

In the pairwise comparisons (Table 4), lesion load significantly mediated GMF differences in both B-MS versus W-MS (total effect $\eta_p^2 = -1.81$, $p < 0.001$; direct effect

$\eta_p^2 = -0.93$, $p < 0.01$; indirect effect $\eta_p^2 = -0.88$, $p < 0.001$; Pm = 48.6%), and H-MS vs W-MS (total effect $\eta_p^2 = -1.09$, $p < 0.01$; direct effect $\eta_p^2 = -0.47$, $p > 0.05$; indirect effect $\eta_p^2 = -0.62$, $p < 0.001$; Pm = 56.9%). Both pairwise comparisons demonstrated significant structural disconnectivity effects in DGM, insular, and anterior cingulate components, while the H-MS versus W-MS comparison additionally showed mediation effects in posterior cingulate, precuneus, and temporal components.

Discussion

This study uniquely combines various neuroimaging analysis techniques aimed at providing a comprehensive assessment of the ethnoracial disparities in MS focusing on GM atrophy. Our results underscore significant ethnoracial disparities in GM atrophy in PwMS, with some of these differences being mediated by WM lesions and consequent structural disconnectivity. This analysis sheds light on disparities in degenerative MS outcomes and the potential underlying mechanisms, underscoring the importance of considering ethnoracial factors in MS research and clinical practice.

Our results show that B-MS and H-MS exhibit lower GMF, and greater lesion burden compared to W-MS. The pattern of GM atrophy topographically aligns with previous studies in MS,[40] and suggests that ethnoracial factors may influence the extent and pattern of neurodegeneration. Notably, B-MS patients showed the most pronounced atrophy in the posterior cingulate, precuneus, and temporal regions, while H-MS patients exhibited greater decreases in the temporooccipital, posterior cingulate, and frontal regions. These patterns suggest that specific GM regions are differentially affected across ethnoracial groups, potentially contributing to the variability in functional clinical outcomes observed in MS.[4] The largest differences in lesion-related structural disconnectivity were observed in the hippocampus, cingulate, precuneus, and deep gray matter, regions known to be critical hubs in the brain's network and heavily impacted by MS pathology.[41–44] Structural disconnectivity, driven by lesion burden and distribution, emerged as a significant mediator of some of the observed GM atrophy differences, echoing the hypothesis that MS-related lesions disrupt the connectivity of neural networks through white matter pathways, leading to secondary neurodegeneration in connected GM regions.[15–17] The mediation effects were particularly notable in the deep gray matter, insular and anterior cingulate GM regions.

Although the groups showed no significant differences in disability as quantified by EDSS, they exhibited significant differences in lesion load, global GM atrophy, and its patterns. This can be explained by the nature of lesion
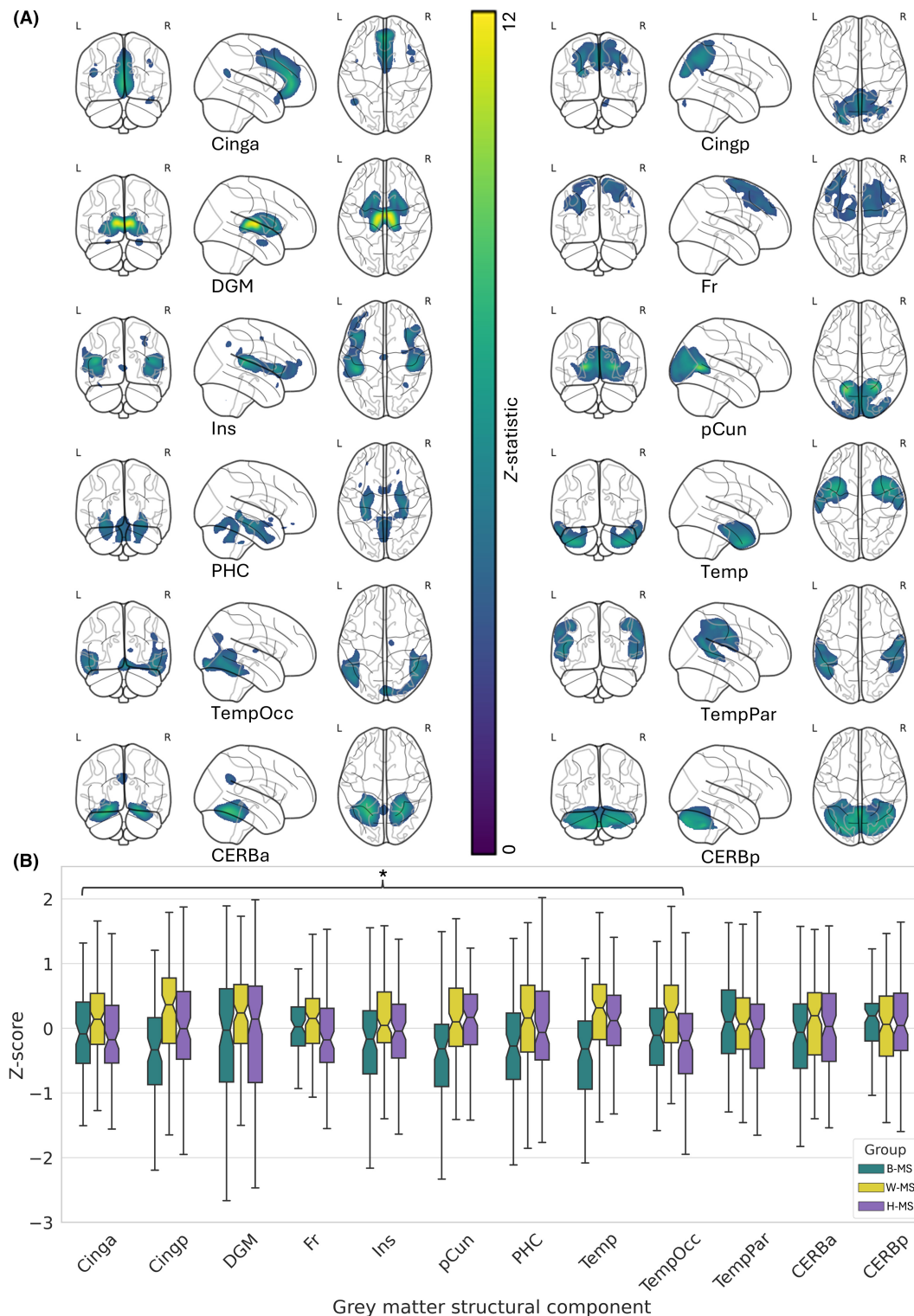
Figure 4. Multivariate gray matter assessment and group differences. (A) Topographic distribution of GMCs identified using SBM. (B) Group differences in the identified GMCs. GMCs with significant group differences are denoted by an asterisk. CERBa, anterior cerebellar component; CERBp, posterior cerebellar component; Cinga, anterior cingulate component; Cingp, posterior cingulate component; DGM, deep gray matter component; Fr, frontal component; Ins, insular component; pCun, precuneus component; PHC, parahippocampal component; Temp, temporal component; TempOcc, temporooccipital component; TempPar, temporoparietal component.

Table 2. Group differences in gray matter atrophy patterns and their lesion-driven structural disconnectivity.

Differences in GM atrophy in the identified components (GMCs)[a]

GMC	F-statistic	η_p^2	p_{FDR}	B-MS < W-MS		B-MS < H-MS		H-MS < W-MS	
				t-statistic	p-value	t-statistic	p-value	t-statistic	p-value
Cinga	7.3	0.05	0.002	−5	<0.001	−1.9	0.1	−3	0.01
Cingp	19.6	0.12	<0.001	−8.5	<0.001	−4.3	<0.001	−3.8	<0.001
DGM	3.8	0.03	0.03	−3.9	<0.001	−1.1	0.5	−2.9	0.01
Fr	5.2	0.03	0.009	−3.5	0.002	−0.1	1	−3.6	0.001
Ins	6.4	0.04	0.003	−4.9	<0.001	−2.5	0.03	−2.3	0.07
pCun	21.6	0.13	<0.001	−7.8	<0.001	−5.7	<0.001	−1.9	0.1
PHC	7.3	0.05	0.002	−6.5	<0.001	−3	0.008	−3	0.007
Temp	23.1	0.14	<0.001	−7.6	<0.001	−5	<0.001	−2.9	0.01
TempOcc	15.6	0.1	<0.001	−6	<0.001	−0.3	0.9	−5.9	<0.001
TempPar	1.9	0.01	0.2	–	–	–	–	–	–
CERBa	2.3	0.02	0.1	–	–	–	–	–	–
CERBp	0.8	0.01	0.4	–	–	–	–	–	–

Differences in structural connectivity to GMCs[b]

GMC	χ^2	p_{FDR}	B-MS > W-MS		B-MS > H-MS		H-MS > W-MS	
			W-statistic	p-value	W-statistic	p-value	W-statistic	p-value
Cinga	11.1	0.02	−4.2	0.008	−0.5	0.9	−3.7	0.02
Cingp	11.2	0.05	−4.3	0.007	−0.5	0.9	−3.7	0.03
DGM	10.6	0.02	−4.2	0.009	−0.6	0.9	−3.6	0.03
Fr	7.5	0.03	−3.6	0.03	−0.9	0.8	−2.9	0.1
Ins	8.2	0.02	−3.7	0.03	−0.7	0.9	−3.1	0.07
pCun	9.5	0.01	−4.1	0.01	−0.7	0.9	−3.2	0.06
PHC	9.7	0.02	−4	0.01	−0.5	0.9	−3.4	0.04
Temp	4.7	0.1	–	–	–	–	–	–
TempOcc	9.1	0.02	−4.1	0.01	−1.1	0.7	−3	0.09
TempPar	10	0.02	−4.2	0.008	−1	0.8	−3.2	0.06
CERBa	10.4	0.02	−4.2	0.008	−0.8	0.8	−3.4	0.04
CERBp	1.2	0.6	–	–	–	–	–	–

B-MS, non-Hispanic Black PwMS group; CERBa, anterior cerebellar component; CERBp, posterior cerebellar component; Cinga, anterior cingulate component; Cingp, posterior cingulate component; DGP, deep gray matter component; Fr, frontal component; GMC, gray matter component; H-MS, Hispanic PwMS group; Ins, insular component; pCun, precuneus component; p_{FDR}, false-discovery rate adjusted p-value; PHC, parahippocampal component; Temp, temporal component; TempOcc, temporooccipital component; TempPar, temporoparietal component; W-MS, non-Hispanic White PwMS group; W-statistic, Wilcoxon rank-sum test statistic; η_p^2, partial eta squared; χ^2, Chi-squared statistic.
[a]Calculated using ANCOVA controlling for age, gender and TIV. Post-hoc comparisons were conducted using Games-Howell test.
[b]Calculated using Kruskal–Wallis test. Post-hoc comparisons were conducted using Dwass–Steel–Critchlow–Fligner (DSCF) test.

topography, which showed notable differences in periventricular lesion volume. Periventricular lesions can be particularly clinically ineloquent, possibly due to the extent of cerebral reserve and functional compensation, especially when contrasted to infratentorial lesions.[45–47] Moreover, EDSS can fail to capture sub-threshold neurologic deficits, compared to other more sensitive measurement tools.[48] In context, the exhibited differences might be compensated for by functional cerebral reserve or contributing to subclinical disability not fully expressed in terms of EDSS.

The lack of substantial mediation effects in some of the identified GM components can be explained by several factors. First, we did not assess demyelinating cortical pathology, which can disproportionately affect temporal and parahippocampal regions[49] and contribute to focal GM atrophy. Additionally, we did not systematically include demographic factors from the Social Determinants of Health framework in our analyses. Social adversity has been shown to contribute to and mediate GM atrophy.[50] Future studies incorporating these factors could provide a more comprehensive understanding of the complex interplay between lesion distribution, structural disconnectivity, and GM atrophy in diverse MS populations.
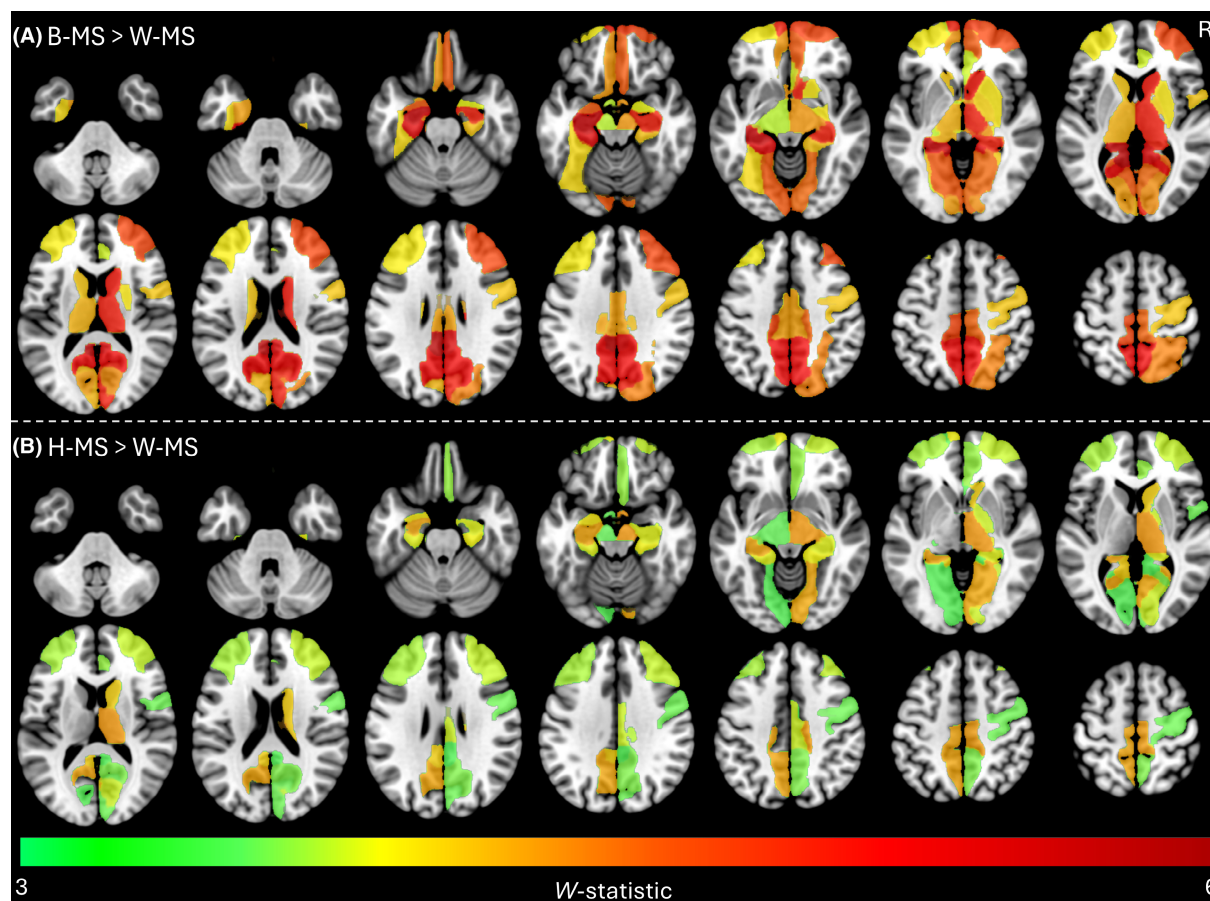
Figure 5. Gray matter disconnectivity group differences. Depicting pair-wise differences in regional gray matter structural disconnectivity secondary to WM hyperintense lesions in B-MS versus W-MS (A), and H-MS versus W-MS (B). Higher W-values denote larger differences.

The observed ethnoracial disparities in GM atrophy and structural disconnectivity have important implications for management approaches in MS. These findings might not directly translate to clinical disability measured by cross-sectional EDSS, though they might underlie longitudinal decline in related clinical function. Given the more pronounced GM atrophy and higher lesion loads in B-MS and H-MS patients, clinicians might consider earlier and more aggressive treatment initiation for these groups. This could involve prioritizing high-efficacy DMTs aimed at curbing lesion formation and neurodegeneration,[51] potentially controlling silent progression.[52] The specific patterns of GM atrophy and disconnectivity observed in different ethnoracial groups could inform tailored cognitive rehabilitation strategies.[53,54] B-MS patients exhibiting atrophy in temporal, posterior cingulate, and precuneus regions might benefit from interventions targeting attention and memory functions associated with these areas. Similarly, the pronounced frontal GM involvement in H-MS patients suggests a potential need for executive function-focused cognitive interventions.[53–55] Furthermore, the structural disconnectivity findings highlight the importance of preserving white matter integrity, underscoring the value of neuroprotective strategies and remyelinating therapies, which might be particularly crucial for B-MS and H-MS patients.[56] Regular monitoring of GM atrophy through more nuanced MRI techniques could be incorporated into routine clinical care, especially for patients from these higher risk groups, to guide treatment decisions and assess therapy effectiveness.[57] Additionally, these findings emphasize the need for increased representation of diverse ethnoracial groups in clinical trials for MS therapies,[58] ensuring that treatment efficacy and safety are adequately evaluated across different populations. In general, our results support the growing emphasis on personalized medicine approaches in MS management.[59] Lastly, our findings emphasize that health and brain structure disparities should not be solely attributed to biological or genetic differences, as sociocultural risk factors can be more actionable and modifiable.[11] Recent works have highlighted the fundamental impact of such sociocultural factors on health outcomes.[50,60,61]

Table 3. Mediation effects of MS-related lesions and resulting structural disconnectivity on differences in GM atrophy between W-MS and combined B-MS and H-MS groups.

Mediation effects of lesion load on differences in total gray matter fraction

	Indirect effect	Direct effect	R_D^2	p_{FDR}	Total effect	R_T^2	p_{FDR}	Pm%
GMF	−0.75*** (−1.1, −0.42)	−0.68* (−1.22, −0.17)	0.45	9×10^{-33}	−1.43*** (−2.02, −0.85)	0.59	4×10^{-49}	52.42

Mediation effects of structural disconnectivity on group differences in gray matter atrophy patterns

GMC	Indirect effect	Direct effect	R_D^2	p_{FDR}	Total effect	R_T^2	p_{FDR}	Pm%
Cing-a	−0.08** (−0.14, −0.03)	−0.25** (−0.4, −0.09)	0.59	1×10^{-48}	−0.33*** (−0.49, −0.16)	0.62	6×10^{-53}	24.30
Cing-p	−0.08** (−0.15, −0.02)	−0.39*** (−0.6, −0.2)	0.40	2×10^{-26}	−0.47*** (−0.68, −0.27)	0.44	5×10^{-30}	16.68
DGM	−0.27*** (−0.42, −0.12)	−0.06 (−0.2, 0.08)	0.34	7×10^{-21}	−0.33** (−0.53, −0.12)	0.70	2×10^{-66}	82.87
Fr	−0.04* (−0.09, −0.003)	−0.17* (−0.33, −0.02)	0.62	7×10^{-53}	−0.21** (−0.37, −0.05)	0.63	4×10^{-54}	16.88
Ins	−0.09** (−0.16, −0.03)	−0.22* (−0.39, −0.04)	0.47	6×10^{-34}	−0.31*** (−0.49, −0.13)	0.53	6×10^{-40}	29.61
pCun	−0.06* (−0.11, −0.02)	−0.21* (−0.38, −0.04)	0.55	2×10^{-43}	−0.27** (−0.45, −0.1)	0.58	6×10^{-47}	23.16
PHC	0.03 (−0.01, 0.08)	−0.33*** (−0.53, −0.12)	0.47	1×10^{-33}	−0.3** (−0.48, −0.1)	0.47	2×10^{-33}	–
Temp	−0.04* (−0.1, −0.002)	−0.39*** (−0.58, −0.19)	0.46	4×10^{-33}	−0.43*** (−0.62, −0.24)	0.48	4×10^{-34}	9.72
TempOcc	−0.02 (−0.05, 0.01)	−0.47*** (−0.67, −0.28)	0.52	2×10^{-39}	−0.49*** (−0.67, −0.31)	0.52	3×10^{-39}	–

Values represent point estimates and 95% confidence intervals.
B-MS, non-Hispanic Black PwMS group; Cing-a, anterior cingulate component; Cing-p, posterior cingulate component; DGM, deep gray matter component; Fr, frontal component; GMC, gray matter component; GMF, gray matter fraction; H-MS, Hispanic PwMS group; Ins, insular component; pCun, precuneus component; PHC, parahippocampal component; Pm%, percent mediated; Temp, temporal component; TempOcc, temporooccipital component.; W-MS, non-Hispanic White PwMS group.
*$p < 0.05$.
**$p < 0.01$.
***$p < 0.001$.

Further research is needed to elucidate the biological, genetic, and environmental factors contributing to the observed ethnoracial disparities in MS. Longitudinal studies examining the progression of GM atrophy and structural disconnectivity over time in diverse populations will be crucial for understanding the dynamic nature of these differences. Additionally, exploring the socioeconomic and healthcare access factors that may underlie these disparities will provide a more comprehensive understanding of the disease process, and possibly inform more equitable healthcare practices and effective management of MS.

Strengths

In this study, we strived to create a balanced cohort of PwMS, ensuring equal representation across diverse ethnoracial groups. Additionally, included participants did not exhibit significant differences in key confounding variables such as age, sex, disease duration, and other relevant clinical parameters minimizing bias and enhancing the validity of our findings. Our cohort underwent both clinical and radiological examinations at the same center, minimizing bias associated with variations in care providers, different MRI systems, and acquisition protocols. Furthermore, we employed both univariate and multivariate techniques to ensure the robustness of our findings.

Limitations

A principal limitation of this study is the absence of a normative healthy control group, which restricts our ability to contextualize the observed gray matter atrophy against a baseline of healthy brain anatomy. Nevertheless, the primary objective was to elucidate ethnoracial

Table 4. Mediation effects of MS-related lesions and resulting structural disconnectivity on differences in GM atrophy in B-MS and H-MS compared to W-MS.

Mediation effects of lesion load on pair-wise differences in GMF

	B-MS versus W-MS				H-MS versus W-MS			
	Indirect effect	Direct effect	Total effect	Pm%	Indirect effect	Direct effect	Total effect	Pm%
GMF	−0.88*** (−1.32, −0.48)	−0.93** (−1.59, −0.29)	−1.81*** (−2.56, −1.07)	48.62	−0.62*** (−1.03, −0.26)	−0.47 (−1.11, 0.14)	−1.09** (−1.76, −0.42)	56.88

Mediation effects of structural disconnectivity on pair-wise differences in GMCs

	B-MS versus W-MS				H-MS versus W-MS			
GMC	Indirect effect	Direct effect	Total effect	Pm%	Indirect effect	Direct effect	Total effect	Pm%
Cing-a	−0.08* (−0.15, −0.02)	−0.3** (−0.49, −0.1)	−0.37*** (−0.57, −0.17)	21.62	−0.08** (−0.15, −0.03)	−0.21* (−0.39, −0.04)	−0.29** (−0.48, −0.11)	27.59
Cing-p	−0.07 (−0.14, −0.004)	−0.68*** (−0.93, −0.45)	−0.75*** (−0.99, −0.51)	–	−0.1** (−0.18, −0.03)	−0.17 (−0.38, 0.05)	−0.26* (−0.47, −0.04)	38.46
DGM	−0.26** (−0.43, −0.08)	−0.12 (−0.29, 0.04)	−0.38** (−0.61, −0.14)	68.42	−0.28** (−0.47, −0.1)	0 (−0.17, 0.15)	−0.29* (−0.53, −0.06)	96.55
Fr	−0.04 (−0.08, −0.001)	−0.04 (−0.22, 0.14)	−0.08 (−0.26, 0.11)	–	−0.04 (−0.09, −0.001)	−0.28** (−0.46, −0.11)	−0.31*** (−0.49, −0.13)	–
Ins	−0.08* (−0.16, −0.01)*	−0.33** (−0.53, −0.12)	−0.41*** (−0.63, −0.19)	19.51	−0.1** (−0.18, −0.02)	−0.13 (−0.33, 0.07)	−0.23* (−0.44, −0.02)	43.48
pCun	−0.06 (−0.12, −0.004)	−0.52*** (−0.73, −0.32)	−0.58*** (−0.79, −0.37)	–	−0.07* (−0.13, −0.02)	0.04 (−0.14, 0.22)	−0.03 (−0.21, 0.15)	–
PHC	0.02 (−0.01, 0.06)	−0.52*** (−0.73, −0.28)	−0.5*** (−0.71, −0.27)	–	0.03 (−0.01, 0.09)	−0.18 (−0.39, 0.05)	−0.15 (−0.36, 0.07)	–
Temp	−0.03 (−0.09, 0.003)	−0.69*** (−0.92, −0.45)	−0.72*** (−0.94, −0.49)	–	−0.06* (−0.14, −0.004)	−0.15 (−0.37, 0.04)	−0.21* (−0.42, −0.001)	28.57
TempOcc	−0.02 (−0.05, 0.01)	−0.39*** (−0.62, −0.17)	−0.41*** (−0.62, −0.19)	–	−0.02 (−0.06, 0.01)	−0.54*** (−0.75, −0.33)	−0.56*** (−0.76, −0.36)	–

Values represent point estimates and 95% confidence intervals.

B-MS, non-Hispanic Black PwMS group; Cing-a, anterior cingulate component; Cing-p, posterior cingulate component; DGM, deep gray matter component; Fr, frontal component; GMC, gray matter component; GMF, gray matter fraction; H-MS, Hispanic PwMS group; Ins, insular component; pCun, precuneus component; PHC, parahippocampal component; Pm%, percent mediated; Temp, temporal component; TempOcc, temporoccipital component.; W-MS, non-Hispanic White PwMS group.

*p < 0.05.
**p < 0.01.
***p < 0.001.

disparities in gray matter atrophy in B-MS and H-MS, using W-MS as a referent group. Determination of ethnoracial group was limited to self-reporting, thus it might not fully encompass biologic factors and genetic background. Social confounders including education, health care access, community, economic stability, and lifestyle were not explored in this study. This retrospective analysis may be constrained by its inability to encompass all pertinent variables and to prospectively control potential unrecognized confounders, and by potentially not accounting for relevant undocumented comorbidities. The use of cross-sectional data limits our ability to infer causality or track the temporal progression of gray matter atrophy. Longitudinal studies are essential to clarify the dynamics and causative factors of these changes more

definitively. Finally, the lack of validated standardized brain templates for minority populations might affect the interpretation of the results, albeit it has been previously shown that the choice of template does not introduce significant differences when using CAT12 for image normalization,[62] and the Human Connectome Project dataset used for the disconnectometry analysis strived to include a representative sample reflecting the ethnoracial diversity in the United States.[63]

Conclusions

This study highlights significant ethnoracial disparities in GM atrophy among PwMS, with lesion-driven structural disconnectivity serving as a significant mediator. The

findings demonstrate more evident gray matter atrophy in Hispanic/Latinx and non-Hispanic Black PwMS when compared to non-Hispanic White PwMS. These disparities emphasize the critical need for tailored diagnostic and therapeutic approaches that consider ethnoracial factors. Moving forward, comprehensive longitudinal studies are necessary to better understand the progression and causative factors behind these disparities. exploring the influence of genetic, environmental, and socioeconomic variables will be vital in developing more effective, personalized MS management strategies.

Acknowledgements

Conflict of Interest

J.A.L. is supported by Bartels Family Endowment, Iglesias Family Foundation, and Brass Family Foundation. J.S.W. holds royalties for monoclonal antibodies out-licensed through UTHealth Houston to Millipore. J.S.W has received compensation for consulting, scientific advisory boards, or other activities with the Cleveland Clinic Foundation, EMD Serono, Inmagene, Novartis, Roche/Genentech, Sandoz, and Zenas. J.S.W. has received compensation as a member of the data safety monitoring or advisory boards from the Cleveland Clinic Foundation, EMD Serono, and Novartis. C.A.P. has received postgraduate fellowship support from Genentech and has participated in advisory boards for Sanofi. C.M.O. has received postgraduate fellowship support from the National MS Society (Sylvia Lawry Grant). C.M.O has received presenting honorarium from the American Academy of Neurology. A.B., J.A.T., B.R.A., J.J., and K.M.H have nothing to disclose.

Author Contributions

A.B. and J.A.L. contributed to the conception and design of the study. A.B., J.A.T., J.J., B.R.A, C.M.O., C.A.P., and J.A.L. contributed to acquisition and analysis of data. A.B., K.M.H., J.S.W., and J.A.L. contributed to drafting a significant portion of the manuscript and preparing figures.

Data Availability Statement

Raw data was generated at UTHealth. Anonymized derived data may be shared upon reasonable request to the corresponding or senior authors with researchers who provide a methodologically sound non-commercial proposal, subject to restrictions according to participant consent and data protection legislation.

References

1. Wallin MT, Culpepper WJ, Campbell JD, et al. The prevalence of MS in the United States: a population-based estimate using health claims data. Neurology. 2019;92: e1029-e1040. doi:10.1212/wnl.0000000000007035

2. Jakimovski D, Bittner S, Zivadinov R, et al. Multiple sclerosis. Lancet. 2024;403:183-202. doi:10.1016/S0140-6736(23)01473-3

3. Hittle M, Culpepper WJ, Langer-Gould A, et al. Population-based estimates for the prevalence of multiple sclerosis in the United States by race, ethnicity, age, sex, and geographic region. JAMA Neurol. 2023;80:693-701. doi:10.1001/jamaneurol.2023.1135

4. Amezcua L, Rivera VM, Vazquez TC, Baezconde-Garbanati L, Langer-Gould A. Health disparities, inequities, and social determinants of health in multiple sclerosis and related disorders in the US: a review. JAMA Neurol. 2021;78:1515-1524. doi:10.1001/jamaneurol.2021.3416

5. Williams MJ, Orlando C, Akisanya J, Amezcua L. Multiple sclerosis in black and Hispanic populations: serving the underserved. Neurol Clin. 2024;42:295-317. doi:10.1016/j.ncl.2023.06.005

6. Orlando CM, Pérez CA, Agyei P, et al. Social determinants of health and disparate disability accumulation in a cohort of black, Hispanic, and white patients with multiple sclerosis. Mult Scler. 2023;29:1304-1315. doi:10.1177/13524585231185046

7. Pérez CA, Lincoln JA. Racial and ethnic disparities in treatment response and tolerability in multiple sclerosis: a comparative study. Mult Scler Relat Disord. 2021;56:103248. doi:10.1016/j.msard.2021.103248

8. Al-Kawaz M, Monohan E, Morris E, et al. Differential impact of multiple sclerosis on cortical and deep gray matter structures in African Americans and Caucasian Americans. J Neuroimaging. 2017;27:333-338. doi:10.1111/jon.12393

9. Pérez CA, Salehbeiki A, Zhu L, Wolinsky JS, Lincoln JA. Assessment of racial/ethnic disparities in volumetric MRI correlates of clinical disability in multiple sclerosis: a preliminary study. J Neuroimaging. 2021;31:115-123. doi:10.1111/jon.12788

10. Nathoo N, Zeydan B, Neyal N, Chelf C, Okuda DT, Kantarci OH. Do magnetic resonance imaging features differ between persons with multiple sclerosis of various races and ethnicities? Front Neurol. 2023;14:1215774. doi:10.3389/fneur.2023.1215774

11. Rivas-Rodríguez E, Amezcua L. Ethnic considerations and multiple sclerosis disease variability in the United States. Neurol Clin. 2018;36:151-162. doi:10.1016/j.ncl.2017.08.007

12. Mey GM, Mahajan KR, DeSilva TM. Neurodegeneration in multiple sclerosis. WIREs Mech Dis. 2023;15:e1583. doi:10.1002/wsbm.1583

13. Hulst HE, Geurts JJG. Gray matter imaging in multiple sclerosis: what have we learned? BMC Neurol. 2011;11:153. doi:10.1186/1471-2377-11-153

14. Eshaghi A, Prados F, Brownlee WJ, et al. Deep gray matter volume loss drives disability worsening in multiple sclerosis. Ann Neurol. 2018;83:210-222. doi:10.1002/ana.25145

15. Tóth E, Szabó N, Csete G, et al. Gray matter atrophy is primarily related to demyelination of lesions in multiple sclerosis: a diffusion tensor imaging MRI study. Front Neuroanat. 2017;11:23. doi:10.3389/fnana.2017.00023

16. Bussas M, Grahl S, Pongratz V, et al. Gray matter atrophy in relapsing-remitting multiple sclerosis is associated with white matter lesions in connecting fibers. Mult Scler J. 2022;28:900-909. doi:10.1177/13524585211044957

17. Lie IA, Weeda MM, Mattiesing RM, et al. Relationship between white matter lesions and gray matter atrophy in multiple sclerosis. Neurology. 2022;98:e1562-e1573. doi:10.1212/WNL.0000000000200006

18. Calabrese M, Preziosa P, Scalfari A, et al. Determinants and biomarkers of progression independent of relapses in multiple sclerosis. Ann Neurol. 2024;96:1-20. doi:10.1002/ana.26913

19. Schoonheim MM, Geurts JJG. What causes deep gray matter atrophy in multiple sclerosis? Am J Neuroradiol. 2019;40:107-108. doi:10.3174/ajnr.A5942

20. Good CD, Johnsrude IS, Ashburner J, Henson RNA, Friston KJ, Frackowiak RSJ. A voxel-based morphometric study of ageing in 465 Normal adult human brains. NeuroImage. 2001;14:21-36. doi:10.1006/nimg.2001.0786

21. Geurts JJG, Calabrese M, Fisher E, Rudick RA. Measurement and clinical effect of grey matter pathology in multiple sclerosis. Lancet Neurol. 2012;11:1082-1092. doi:10.1016/S1474-4422(12)70230-2

22. Amiri H, de Sitter A, Bendfeldt K, et al. Urgent challenges in quantification and interpretation of brain grey matter atrophy in individual MS patients using MRI. NeuroImage: Clinical. 2018;19:466-475. doi:10.1016/j.nicl.2018.04.023

23. Singh S, Tench CR, Tanasescu R, Constantinescu CS. Localised Grey matter atrophy in multiple sclerosis and clinically isolated syndrome—a coordinate-based meta-analysis, meta-analysis of networks, and meta-regression of voxel-based morphometry studies. Brain Sci. 2020;10:798.

24. MacKenzie-Graham A, Kurth F, Itoh Y, et al. Disability-specific atlases of gray matter loss in relapsing-remitting multiple sclerosis. JAMA Neurol. 2016;73:944-953. doi:10.1001/jamaneurol.2016.0966

25. Rocca MA, Valsasina P, Meani A, et al. Association of Gray Matter Atrophy Patterns with Clinical Phenotype and Progression in multiple sclerosis. Neurology. 2021;96:e1561-e1573. doi:10.1212/WNL.0000000000011494

26. Xu L, Groth KM, Pearlson G, Schretlen DJ, Calhoun VD. Source-based morphometry: the use of independent component analysis to identify gray matter differences with application to schizophrenia. Hum Brain Mapp. 2009;30:711-724. doi:10.1002/hbm.20540

27. Mollenhauer B, Zimmermann J, Sixel-Doring F, et al. Baseline predictors for progression 4 years after Parkinson's disease diagnosis in the De novo Parkinson cohort (DeNoPa). Mov Disord. 2019;34:67-77, 77. doi:10.1002/mds.27492

28. Tozlu C, Jamison K, Gu Z, et al. Estimated connectivity networks outperform observed connectivity networks when classifying people with multiple sclerosis into disability groups. Neuroimage Clin. 2021;32:102827. doi:10.1016/j.nicl.2021.102827

29. Kuceyeski A, Maruta J, Relkin N, Raj A. The network modification (NeMo) tool: elucidating the effect of white matter integrity changes on cortical and subcortical structural connectivity. Brain Connect. 2013;3:451-463. doi:10.1089/brain.2013.0147

30. Baron RM, Kenny DA. The moderator-mediator variable distinction in social psychological research: conceptual, strategic, and statistical considerations. J Pers Soc Psychol. 1986;51:1173-1182. doi:10.1037//0022-3514.51.6.1173

31. Michaelson NM, Rúa SH, Kaunzner UW, et al. Impact of paramagnetic rim lesions on disability and race in multiple sclerosis: mediation analysis. Ann Clin Transl Neurol. 2024;11:2923-2931. doi:10.1002/acn3.52203

32. Wiltgen T, McGinnis J, Schlaeger S, et al. LST-AI: a deep learning ensemble for accurate MS lesion segmentation. Neuroimage Clin. 2024;42:103611. doi:10.1016/j.nicl.2024.103611

33. Valverde S, Oliver A, Lladó X. A white matter lesion-filling approach to improve brain tissue volume measurements. Neuroimage Clin. 2014;6:86-92. doi:10.1016/j.nicl.2014.08.016

34. Pirzada S, Uddin MN, Figley TD, et al. Spatial normalization of multiple sclerosis brain MRI data depends on analysis method and software package. Magn Reson Imaging. 2020;68:83-94. doi:10.1016/j.mri.2020.01.016

35. Guo C, Ferreira D, Fink K, Westman E, Granberg T. Repeatability and reproducibility of FreeSurfer, FSL-SIENAX and SPM brain volumetric measurements and the effect of lesion filling in multiple sclerosis. Eur Radiol. 2019;29:1355-1364. doi:10.1007/s00330-018-5710-x

36. Gilmore AD, Buser NJ, Hanson JL. Variations in structural MRI quality significantly impact commonly used measures of brain anatomy. Brain Inform. 2021;8:7. doi:10.1186/s40708-021-00128-2

37. Spisák T, Spisák Z, Zunhammer M, et al. Probabilistic TFCE: a generalized combination of cluster size and voxel intensity to increase statistical power. NeuroImage. 2019;185:12-26. doi:10.1016/j.neuroimage.2018.09.078

38. Lee TW, Girolami M, Sejnowski TJ. Independent component analysis using an extended infomax algorithm for mixed subgaussian and supergaussian sources. Neural Comput. 1999;11:417-441. doi:10.1162/089976699300016719

39. Rosseel Y. Lavaan: an R package for structural equation modeling. J Stat Softw. 2012;48:1-36. doi:10.18637/jss.v048.i02

40. Eshaghi A, Marinescu RV, Young AL, et al. Progression of regional grey matter atrophy in multiple sclerosis. Brain. 2018;141:1665-1677. doi:10.1093/brain/awy088

41. Cortese R, Battaglini M, Stromillo ML, et al. Regional hippocampal atrophy reflects memory impairment in patients with early relapsing remitting multiple sclerosis. J Neurol. 2024;271:4897-4908. doi:10.1007/s00415-024-12290-8

42. Cifelli A, Arridge M, Jezzard P, Esiri MM, Palace J, Matthews PM. Thalamic neurodegeneration in multiple sclerosis. Ann Neurol. 2002;52:650-653. doi:10.1002/ana.10326

43. Pagani E, Rocca MA, Gallo A, et al. Regional brain atrophy evolves differently in patients with multiple sclerosis according to clinical phenotype. Am J Neuroradiol. 2005;26:341-346.

44. Ontaneda D, Raza PC, Mahajan KR, et al. Deep grey matter injury in multiple sclerosis: a NAIMS consensus statement. Brain. 2021;144:1974-1984. doi:10.1093/brain/awab132

45. Krieger SC, Cook K, De Nino S, et al. The topographical model of multiple sclerosis: a dynamic visualization of disease course. Neurol Neuroimmunol Neuroinflamm. 2016;3:e279. doi:10.1212/nxi.0000000000000279

46. Mowry EM, Pesic M, Grimes B, Deen S, Bacchetti P, Waubant E. Demyelinating events in early multiple sclerosis have inherent severity and recovery. Neurology. 2009;72:602-608. doi:10.1212/01.wnl.0000342458.39625.91

47. Krieger S, Cook K, Hersh CM. Understanding multiple sclerosis as a disease spectrum: above and below the clinical threshold. Curr Opin Neurol. 2024;37:189-201. doi:10.1097/wco.0000000000001262

48. Krieger SC, Antoine A, Sumowski JF. EDSS 0 is not normal: multiple sclerosis disease burden below the clinical threshold. Mult Scler J. 2022;28:2299-2303. doi:10.1177/13524585221108297

49. Geisseler O, Pflugshaupt T, Bezzola L, et al. The relevance of cortical lesions in patients with multiple sclerosis. BMC Neurol. 2016;16:204. doi:10.1186/s12883-016-0718-9

50. Dumornay NM, Lebois LAM, Ressler KJ, et al. Racial disparities in adversity during childhood and the false appearance of race-related differences in brain structure. Am J Psychiatry. 2023;180:127-138. doi:10.1176/appi.ajp.21090961

51. Filippi M, Amato MP, Centonze D, et al. Early use of high-efficacy disease-modifying therapies makes the difference in people with multiple sclerosis: an expert opinion. J Neurol. 2022;269:5382-5394. doi:10.1007/s00415-022-11193-w

52. Cree BAC, Hollenbach JA, Bove R, et al. Silent progression in disease activity-free relapsing multiple sclerosis. Ann Neurol. 2019;85:653-666. doi:10.1002/ana.25463

53. Calabrese M, Atzori M, Bernardi V, et al. Cortical atrophy is relevant in multiple sclerosis at clinical onset. J Neurol. 2007;254:1212-1220. doi:10.1007/s00415-006-0503-6

54. Steenwijk MD, Geurts JJ, Daams M, et al. Cortical atrophy patterns in multiple sclerosis are non-random and clinically relevant. Brain. 2016;139:115-126. doi:10.1093/brain/awv337

55. Chiaravalloti ND, Genova HM, DeLuca J. Cognitive rehabilitation in multiple sclerosis: the role of plasticity. Front Neurol. 2015;6:67. doi:10.3389/fneur.2015.00067

56. Plemel JR, Liu WQ, Yong VW. Remyelination therapies: a new direction and challenge in multiple sclerosis. Nat Rev Drug Discov. 2017;16:617-634. doi:10.1038/nrd.2017.115

57. Filippi M, Rocca MA, Ciccarelli O, et al. MRI criteria for the diagnosis of multiple sclerosis: MAGNIMS consensus guidelines. Lancet Neurol. 2016;15:292-303. doi:10.1016/s1474-4422(15)00393-2

58. Langer-Gould AM, Gonzales EG, Smith JB, Li BH, Nelson LM. Racial and ethnic disparities in multiple sclerosis prevalence. Neurology. 2022;98:e1818-e1827. doi:10.1212/WNL.0000000000200151

59. Cerqueira JJ, Compston DAS, Geraldes R, et al. Time matters in multiple sclerosis: can early treatment and long-term follow-up ensure everyone benefits from the latest advances in multiple sclerosis? J Neurol Neurosurg Psychiatry. 2018;89:844-850. doi:10.1136/jnnp-2017-317509

60. Llibre-Guerra JJ, Jiang M, Acosta I, et al. Social determinants of health but not global genetic ancestry predict dementia prevalence in Latin America. Alzheimers Dement. 2024;20:4828-4840. doi:10.1002/alz.14041

61. Stulberg EL, Lisabeth L, Schneider ALC, et al. Correlations of socioeconomic and clinical determinants with United States County-level stroke prevalence. Ann Neurol. 2024;96:739-744. doi:10.1002/ana.27039

62. Zhou X, Wu R, Zeng Y, et al. Choice of voxel-based morphometry processing pipeline drives variability in the location of neuroanatomical brain markers. Commun Biol. 2022;5:913. doi:10.1038/s42003-022-03880-1

63. Project HC. Human Connectome Project (HCP) Young Adult - Recruitment. n.d. https://www.humanconnectome.org/study/hcp-young-adult/project-protocol/recruitment

Supporting Information

Additional supporting information may be found online in the Supporting Information section at the end of the article.

Data S1.